THE JOURNAL OF BIOLOGICAL CHEMISTRY VOL. 285, NO. 51, pp. 40322–40332, December 17, 2010
Printed in the U.S.A.

Sphingolipid-mediated Inhibition of Apoptotic Cell Clearance by Alveolar Macrophages*[S]

Received for publication, May 3, 2010, and in revised form, September 23, 2010 Published, JBC Papers in Press, October 18, 2010, DOI 10.1074/jbc.M110.137604

Daniela N. Petrusca[‡], Yuan Gu[‡], Jeremy J. Adamowicz[‡], Natalia I. Rush[‡], Walter C. Hubbard[§], Patricia A. Smith[‡], Evgeni V. Berdyshev[¶], Konstantin G. Birukov[¶], Chao-Hung Lee[‖], Rubin M. Tuder[**], Homer L. Twigg III[‡], R. William Vandivier[**], and Irina Petrache[‡ ‡‡1]

From the [‡]Department of Medicine, Indiana University, Indianapolis, Indiana 46202, the [§]Department of Medicine, Johns Hopkins University, Baltimore, Maryland 21287, the [¶]Department of Medicine, University of Chicago, Chicago, Illinois 60637, the [‖]Department of Pathology and Laboratory Medicine, Indiana University, Indianapolis, Indiana 46202, the [**]Division of Pulmonary Sciences and Critical Care Medicine, University of Colorado, Denver, Colorado 80045, and the [‡‡]R. L. Roudebush Veteran Affairs Medical Center, Indianapolis, Indiana 46202

A decreased clearance of apoptotic cells (efferocytosis) by alveolar macrophages (AM) may contribute to inflammation in emphysema. The up-regulation of ceramides in response to cigarette smoking (CS) has been linked to AM accumulation and increased detection of apoptotic alveolar epithelial and endothelial cells in lung parenchyma. We hypothesized that ceramides inhibit the AM phagocytosis of apoptotic cells. Release of endogenous ceramides via sphingomyelinase or exogenous ceramide treatments dose-dependently impaired apoptotic Jurkat cell phagocytosis by primary rat or human AM, irrespective of the molecular species of ceramide. Similarly, *in vivo* augmentation of lung ceramides via intratracheal instillation in rats significantly decreased the engulfment of instilled target apoptotic thymocytes by resident AM. The mechanism of ceramide-induced efferocytosis impairment was dependent on generation of sphingosine via ceramidase. Sphingosine treatment recapitulated the effects of ceramide, dose-dependently inhibiting apoptotic cell clearance. The effect of ceramide on efferocytosis was associated with decreased membrane ruffle formation and attenuated Rac1 plasma membrane recruitment. Constitutively active Rac1 overexpression rescued AM efferocytosis against the effects of ceramide. CS exposure significantly increased AM ceramides and recapitulated the effect of ceramides on Rac1 membrane recruitment in a sphingosine-dependent manner. Importantly, CS profoundly inhibited AM efferocytosis via ceramide-dependent sphingosine production. These results suggest that excessive lung ceramides may amplify lung injury in emphysema by causing both apoptosis of structural cells and inhibition of their clearance by AM.

The patchy inflammation in pulmonary emphysema, a major form of chronic obstructive pulmonary disease, has been attributed to a direct effect of cigarette smoke (CS)[2] and/or pollutants or a subsequent increase in oxidative stress causing enhanced recruitment of inflammatory cells (1). Studies in the past decade revealed that lung parenchyma structural (epithelial and endothelial) cell apoptosis is a key event in emphysema (2–5), but its integration in the inflammatory processes in the lung remains obscure. One mechanism postulated to link apoptosis and inflammation is a defect in clearance of apoptotic cells in the lung, which is normally promptly and efficiently executed via a unique, highly dynamic, and regulated phagocytic process of central importance for tissue homeostasis (6). An impairment of apoptotic cell phagocytosis (efferocytosis) (7), primarily carried out by specialized phagocytes such as macrophages, may explain the increased detection of apoptotic cells (8) in diseased tissues, such as emphysema lungs (6, 9), and may lead to secondary necrosis of such cells with ensuing inflammation. The relevance of efferocytosis in the context of emphysema has been recently investigated *in vitro* and *in vivo* (6, 10), where studies have shown that macrophages isolated from patients with chronic obstructive pulmonary disease or experimentally exposed to CS exhibited decreased efferocytosis (11, 12). Identifying the mechanisms by which CS exerts its negative effect on efferocytosis is of high importance to ultimately rebalancing the homeostatic clearance of apoptotic cells and harnessing inflammation in emphysema lungs.

Ceramides are signaling sphingolipids serving as second messengers for functions ranging from differentiation to growth arrest and apoptosis (13). Ceramide levels are regulated through hydrolysis of sphingomyelin by sphingomyelinases (SMases), through *de novo* ceramide synthesis (14, 15) via serine palmitoyl-CoA transferase (SPT) and ceramide synthases, or through ceramidase-regulated catabolism to sphingosine (16). Our previous investigations showed that ceramide synthesis is increased in the whole lung in response to CS and oxidative stress and that increased ceramides contribute to apoptosis of lung parenchyma (epithelial and endothe-

* This work was supported, in whole or in part, by National Institutes of Health Grant 1 S10 RR16798 (to W. C. H. for funding the API4000 LC-MS/MS system). This work was also supported by American Heart Association Grants 0826103G (to D. N. P.) and RO1HL077328 (to I. P.).

[S] The on-line version of this article (available at http://www.jbc.org) contains supplemental Fig. S1.

[1] To whom correspondence should be addressed: Indiana University, Division of Pulmonary, Allergy, Critical Care and Occupational Medicine, Walther Hall-R3 C400, 980 W. Walnut St., Indianapolis, IN 46202-5120. Tel.: 317-94-2894; Fax: 317-278-7030; E-mail: ipetrach@iupui.edu.

[2] The abbreviations used are: CS, cigarette smoking/smoke; AM, alveolar macrophages; SMase, sphingomyelinase; SPT, serine palmitoyl-CoA transferase; DHC, dihydroceramide; BAL, bronchoalveolar lavage; PI, propidium iodide; AC, air control; MAPP, (1*S*,2*R*)-D-erythro-2-(*N*-myristoylamino)-1-phenyl-1-propanol; Cer, ceramide; S1P, sphingosine-1-phosphate.

lial) cells in emphysema models while inducing AM accumulation (17). Because AM are resistant to ceramide-induced apoptosis (18), we hypothesized that ceramides inhibit the AM phagocytic function of apoptotic cells.

Little is known about the role of ceramides in the phagocytosis of apoptotic cells, although several components of the sphingolipid metabolism have been implicated in cellular processes related to Fc- and complement-dependent phagocytosis. For instance, the acid SMase has been shown to be required for efficient phagolysosomal fusion (19, 20), whereas ceramide-1-phosphate, a phosphorylation product of ceramide, has been implicated in the regulation of macrophage survival and neutrophil phagocytic function (21). The role of ceramide in the signal transduction of efferocytosis and its involvement in the mechanisms by which CS impairs AM efferocytosis are not known. The Rho family GTPases and their downstream effectors, traditionally linked to cytoskeletal reorganization (22), have a profound role in differentially modulating phagocytosis, because Rac1 and Cdc42 activate, whereas RhoA inhibits efferocytosis (23). Although ceramides may activate RhoA and facilitate its plasma membrane translocation required for ceramide-induced actin stress fiber formation in fibroblasts (24), their effect on Rho-GTPases in AM has not been reported.

Our work, using primary AM *ex vivo*, as well as *in vivo* studies of resident AM in rats, shows that ceramides markedly impair the ability of AM to engulf apoptotic cells through a mechanism that involves sphingosine generation and modulation of Rac1 availability.

EXPERIMENTAL PROCEDURES

Reagents—All of the chemical reagents were purchased from Sigma-Aldrich unless otherwise stated. Ceramides with short (C6:0; C8:0) or intermediate (C16:0) fatty acid chain, dihydroceramide (DHC; 6:0), polyethylene glycol-conjugated ceramide C16:0-PEG 2000, as well as brain ceramides mixture were purchased from Avanti Polar Lipids (Alabaster, AL).

Cell Lines—Human acute T cell leukemia cell line Jurkat (ATCC) was maintained in complete culture medium consisting of RPMI 1640 supplemented with heat-inactivated fetal bovine serum (10%), penicillin (100 units/ml), and streptomycin (0.1 mg/ml). The rat alveolar macrophage cell line NR8383 (ATCC) was maintained in Ham's F12K medium containing L-glutamine (2 mM), sodium bicarbonate (1.5 g/liter), and heat-inactivated fetal bovine serum (15%).

Primary Human AM—The human acellular bronchoalveolar lavage (BAL) fluid and human AM were obtained via bronchoscopy, following a protocol approved by the institutional review board for human research at Indiana University Purdue University, Indianapolis. The procedure was performed under conscious sedation through a fiberoptic bronchoscope wedged in subsegmental bronchi of the right middle lobe or lingula, as described previously (25), instilling 300 ml of sterile saline (0.9% NaCl) and obtaining at least a 50% return. Lavage fluid was filtered through sterile gauze, and BAL cells were pelleted by centrifugation. The supernatant was saved as acellular BAL fraction at −70 °C until further testing. AM were resuspended in media and used freshly for phagocytic assays as described below.

Primary Rat AM—Primary rat AM were isolated from Sprague-Dawley rats by BAL, as described previously (26). Rat lungs were lavaged with cold sterile 0.9% NaCl (10 ml three times). Cell counts and viability were determined by trypan blue dye exclusion. The cells were pelleted by centrifugation (250 × *g*; 10 min) and then resuspended in complete medium RPMI 1640 supplemented with fetal bovine serum (10%), sodium pyruvate (1 mM), nonessential amino acids (1%), glucose (14 mM), $NaHCO_3$ (17.9 mM), HEPES (10 mM), penicillin (100 units/ml), and streptomycin (0.1 mg/ml).

Phagocytosis Assay—Primary AM were accommodated in culture for 3 days before phagocytosis experiments. Apoptosis was induced in target Jurkat cells by UV exposure (30 mJ/cm^2, 60 s) followed by incubation for 3.5 h (37 °C and 5% CO_2), a time sufficient to generate late apoptotic, annexin-positive, and PI-positive cells (>70% of the cell population, as detected by dual annexin V/PI staining and flow cytometry). For subsequent experiments, singular PI staining (50 μg/ml, 15 min) was utilized for apoptotic target cells, followed by washing and co-culture at a 1:5 ratio of macrophages to target cells for 1 h. After co-culture, nonengulfed Jurkats were extensively washed with cold PBS, and the AM were harvested by scraping and were fixed with paraformaldehyde (1%). Trypan blue (0.04%) was utilized to differentiate between apoptotic target attachment/binding and intracellular ingestion, following a fluorescence quenching strategy described previously (27). As phagocytosis negative controls, we co-cultured AM with apoptotic targets at 4 °C. Efferocytosis was quantified by flow cytometry utilizing a previously described method (28) and a Cytomics FC500 cytofluorimeter (Beckman Coulter, Fullerton, CA) with CXP software. The results were expressed as efferocytosis index, defined as the percentage of AM that engulfed apoptotic cells relative to the total number of AM or relative phagocytic index, defined as the percentage of treated AM with engulfed apoptotic cells relative to the number of untreated AM with engulfed apoptotic cells (used as a positive control).

CS Extract—Filtered research grade cigarettes (1R3F) from the Kentucky Tobacco Research and Development Center (University of Kentucky, Lexington, KY) were used for preparing an aqueous CS extract. CS (100%) was prepared by bubbling smoke from two cigarettes into 20 ml of PBS at a rate of 1 cigarette/min to 0.5 cm above the filter (29), followed by pH adjustment to 7.4 and 0.2-μm filtration. A similar procedure was followed for the air control (AC) extract preparation but bubbling ambient air rather than CS into the cell culture medium.

Animal Studies—The Animal Care and Use Committee of the Indiana University School of Medicine approved all of the experimental procedures. Male Sprague-Dawley rats were obtained from Charles River Laboratories (Wilmington, MA). Thymocytes were harvested from rats (age 3–4 weeks old) and maintained in culture (RPMI 1640 medium supplemented with 10% FBS and 1% penicillin/streptomycin) for up to 48 h, sufficient for spontaneously undergoing apoptosis. Rats (9–16 weeks old, 300–400 g) were instilled intratrache-

ally with Cer C16:0-PEG 2000 (10 mg/kg) or vehicle (PEG 2000). After 24 h, PI-stained apoptotic rat thymocytes (5×10^7/rat) were instilled intratracheally, and BAL was harvested after 30 min, quenched with trypan blue, and fixed with 1% paraformaldehyde. Efferocytosis was quantified by flow cytometry.

Apoptosis—Target cells (UV-treated Jurkat, rat thymocytes) or AM were stained with annexin V and PI following the manufacturer's protocol (R & D Systems, Minneapolis, MN). Apoptosis was quantified by flow cytometry.

Ceramide Determination—Lipid extraction and total lipid phosphorus (P_i) measurements utilized a modified Bligh and Dyer method (30), followed by P_i labeling with NH_4-molybdate (31), as described previously (17). Sphingolipid analyses were performed via combined LC-MS/MS, using the API4000 Q-trap hybrid triple quadrupole linear ion trap mass spectrometer (Applied Biosystems-Sciex) equipped with turbo ion spray ionization source and Agilent 1100 series liquid chromatography as a front end (Agilent Technologies, Wilmington, DE). The following individual molecular species of ceramides were monitored: 14:0, 16:0, 18:0, 18:1, 20:0, 24:0, and 24:1-ceramides, utilizing C_{17} ceramide as internal standard. Ceramide measurements were normalized by total lipid phosphorus (P_i).

Ceramide Synthesis Inhibition Studies—The following inhibitors were utilized by pretreating rat AM for the indicated time: the ceramide synthase inhibitor fumonisin (FB1; 10 μM, 2 h; Cayman Chemicals, Ann Arbor, MI), the SPT inhibitor myriocin (My; 50 nM; 2 h; Biomol International, Plymouth Meeting, PA), the neutral SMase inhibitor GW4869 (20 μM, 30 min; Calbiochem, San Diego, CA); the acid SMase inhibitor imipramine (50 μM, 1 h) (Calbiochem, San Diego, CA); or the ceramidase inhibitor (1*S*,2*R*)-D-erythro-2-(*N*-myristoylamino)-1-phenyl-1-propanol (MAPP; 1 μM, 2 h; Biomol Int., Plymouth Meeting, PA).

siRNA and Real Time RT-PCR—Rat AM from BAL were cultured onto 12-well plates and transfected with 1 μM of nontarget siRNA oligonucleotides or directed against acid ceramidase (encoded by ASAH1) using Accell Smart Pool siRNA (Dharmacon; Thermo Fisher Scientific Inc., Waltham, MA). After 72 h, total RNA was extracted using RNA isolation kit (Qiagen), and the cDNA was reversely transcripted from 1 μg of total RNA by using the first strand synthesis kit (Invitrogen) with random primers. mRNA expression was quantified using QuantiTect SYBR green RT-PCR kit (Qiagen) and the following primers for ASAH1: sense (5′-GCCGCTTGCAGCTGGGAAGAT-3′) and reverse (5′-GGTGTACCACGGAACTGGTCCTC-3′) and for ASAH2: sense (5′-TGGAGAAGACTTGGGCCTTA-3′) and reverse (5′-TCCAGGCAGATAGCCTCTGT-3′) using a 7500 real time PCR system (Applied Biosystems, Foster City, CA). The results were normalized to rat endogenous cellular GAPDH. The relative expression was assessed by the comparative C_T method correcting for amplification efficiency of the primers and performed in triplicate.

Rac1 Overexpression—NR8383 cells were transiently transfected with pEGFP-C1-Rac1 plasmid DNA (3 μg/10^6 cells or empty vector, using the Amaxa nucleofector system (Lonza, Allendale, NJ), following the Macrophage nucleofector kit protocol (Amaxa Biosystems, Gaithersburg, MD). The cDNA of wild type Rac1 and constitutively active RacV12 mutant were a gift from Gary Bokoch (Scripps, La Jolla, CA). Mammalian expression vector for Rac1-EGFP was prepared by Bakhtiyor Yakubov (University of Chicago) by subcloning full-length cDNA encoding wild type or constitutively activated Rac1 into pEGFP-C1 plasmid (Clontech, CA) using XhoI and BamHI cloning sites. The transfection efficiency was determined microscopically and by flow cytometry.

Rac1 and RhoA Activities—Primary rat AM were assessed utilizing the G-LISA assay kit (Cytoskeleton, Inc., Denver, CO), according to the manufacturer's protocol, and the readouts were analyzed with SpectraMax M2 (Molecular Devices).

Western Blotting—Cellular lysates from the harvested cells were separated into membrane and cytoplasmic fractions, utilizing a membrane extraction kit (BioVision), according to the manufacturer's protocol. Equal protein amounts from each fraction, as determined by BCA protein analysis (Pierce) were separated by SDS-PAGE and transferred onto a PVDF membrane followed by routine immunoblotting, as described previously (17). Immune complexes were detected using ECL or ECL-plus (Amersham Biosciences), quantified by densitometry, and normalized using specific β-actin (1:10000; Sigma), flotillin 2 (1:1,000; Santa Cruz), or CD71 (1:1000; AbD Serotec) antibody.

Immunocytochemistry—After fixation in paraformaldehyde (4%), NR8383 cells were stained for either actin only or for both actin and Rac1 (clone 23A8; Millipore, Billerica, MA), using Texas Red phalloidin (Molecular Probes/Invitrogen) and a Rac1 monoclonal antibody, respectively, followed by Alexa fluor 488 chicken anti-mouse antibody (Molecular Probes/Invitrogen) staining, as described previously (32). The images were obtained using a Nikon H600L fluorescence microscope with a camera and NIS-Elements AR 3.0 software.

Statistical Analysis—Statistical analysis was performed using SigmaStat 3.5. Comparisons among groups were made using analysis of variance. For experiments in which two conditions were being compared, a two-tailed Student's *t* test was used. All of the experiments were performed at least three times, and the data were expressed as the means ± S.E. Statistically significant differences were considered if $p < 0.05$.

RESULTS

Ceramides Inhibit the Apoptotic Clearance Function of Primary AM—Ceramides are sphingolipids that can be released as second messengers intracellularly or can be found extracellular when generated at the plasma membrane or when released in the circulating plasma (33). We have previously demonstrated increased levels of various ceramide species in lung samples from chronic obstructive pulmonary disease patients (17) and in the lungs of mice exposed to CS (34). To test our hypothesis that ceramides inhibit efferocytosis, ceramides were augmented by three approaches: treatment with exogenous bioactive ceramides, which have been routinely used to mimic the function of endogenous ceramides (35–37); generation of endogenous ceramides via sphingomyelin hydrolysis by active neutral SMase treatment; and exposure of

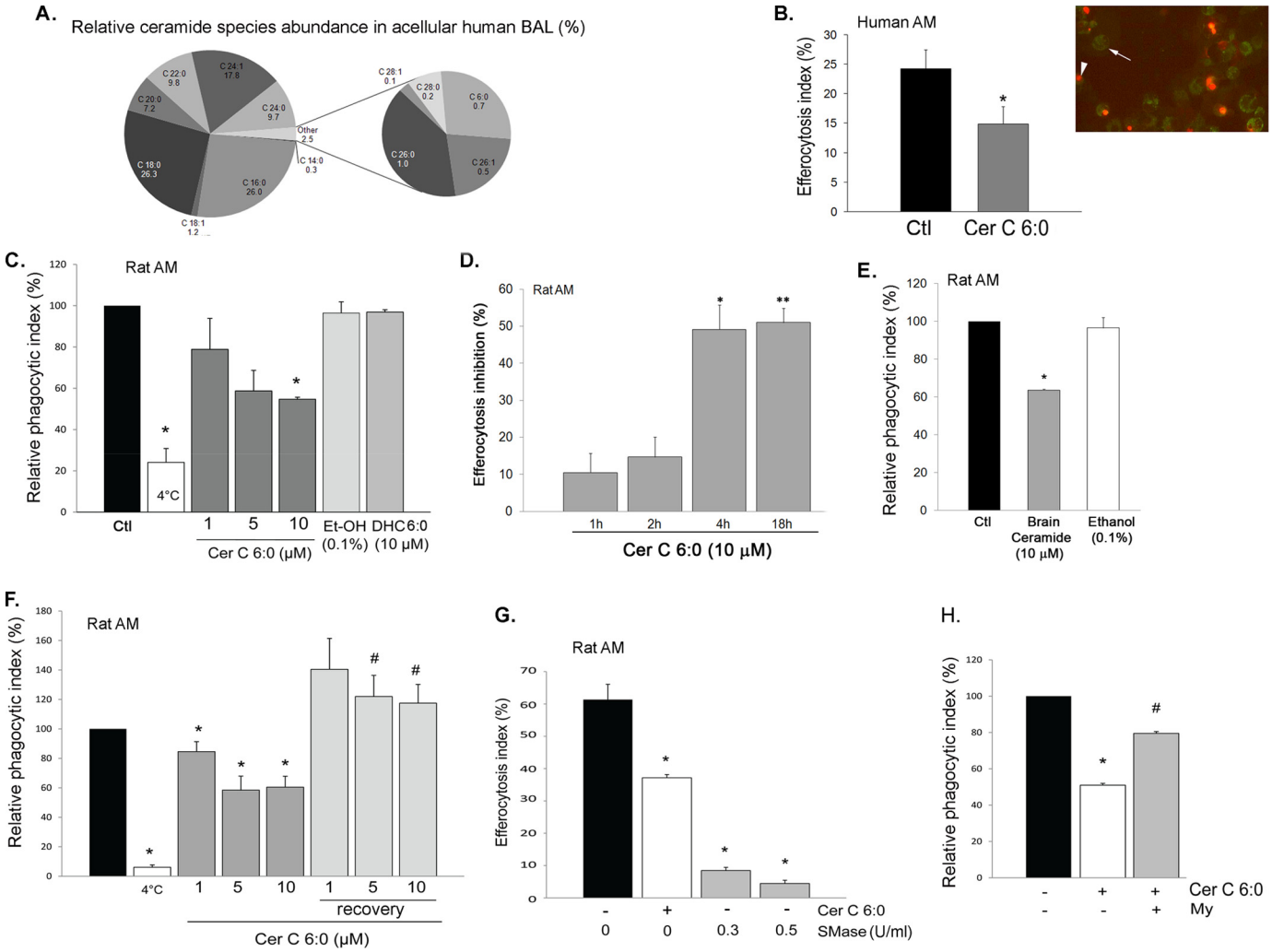

FIGURE 1. **Ceramide inhibits AM efferocytosis *ex vivo*.** *A*, abundance of ceramide species measured in the human BAL acellular fluid by combined LC-MS/MS. The data shown are the averages of $n = 15$ BAL obtained from apparently healthy volunteers. *B–F*, engulfment efficiency of human (*B*) or rat AM was assessed after AM were pretreated with ceramides for 4 h (unless otherwise stated) and co-cultured for 1 h with PI-stained apoptotic Jurkat cells. *B*, quantification of human AM efferocytosis by microscopy. *Right panel*, representative image of AM exhibiting green auto-fluorescence (*arrowhead*) with internalized PI-stained apoptotic Jurkat cells (*red*, *arrow*). *Left panel*, efferocytosis index calculated as the percentage of AM with engulfed PI-stained cells relative to the total AM number, using coded slides (means ± S.E.; *, $p < 0.05$; Student's *t* test) after treatment with vehicle (*Ctl*) or ceramide (Cer 6:0; 10 μM; 4 h). *C* and *D*, dose dependence (*C*; at 4 h) and kinetics (*D*) of inhibitory effect of Cer 6:0, its vehicle ethanol (*Et-OH*), or its precursor DHC (6:0) on rat AM efferocytosis. *C*, efferocytosis was measured by flow cytometry and expressed as relative phagocytic index (percentage of efferocytosis of treated AM relative to that of untreated AM). *White bar*, AM co-incubated with apoptotic Jurkats at 4 °C (mean ± S.E.; $n = 14$; (*, $p < 0.05$ *versus* control). *D*, efferocytosis was measured by flow cytometry and expressed as inhibitory activity (%) compared with untreated AM (mean ± S.E.; $n = 3$; *, $p = 0.007$; **, $p = 0.005$ *versus* control). *E*, rat AM efferocytosis was measured by flow cytometry and expressed as relative phagocytic index (percentage of untreated control: *black bar*) following treatment with brain ceramides (a porcine extract containing long chain ceramides) (10 μM; 4 h) or with vehicle (mean ± S.E.; $n = 3$; *, $p < 0.05$ *versus* control). *F*, effect of post-ceramide recovery of rat AM efferocytosis determined by flow cytometry and expressed as relative phagocytic index (percentage of untreated AM). Rat primary AM were treated with ceramide C6:0 (1, 5, or 10 μM; 4 h) and then allowed to recover overnight in regular growth medium prior to efferocytosis assay (means ± S.E.; $n = 3$; *, $p < 0.05$ *versus* control; #, $p < 0.05$ *versus* corresponding treatments). *G*, rat AM efferocytosis was measured by flow cytometry and expressed as efferocytosis index following treatment (4 h) with active neutral SMase at the indicated concentrations before challenge with apoptotic targets. Treatment with Cer 6:0 (10 μM; 4 h; *white bar*) is shown for comparison (means ± S.E.; $n = 3$; *, $p < 0.05$ *versus* control). *H*, rat AM efferocytosis expressed as relative phagocytic index (percentage of untreated control: *black bar*) following treatment with Cer 6:0 (10 μM; 4 h) after preincubation with myriocin, an inhibitor of SPT in the *de novo* ceramide synthesis pathway (*My*, 50 nM, 2 h; $n = 3$; means ± S.E.; *, $p < 0.05$ *versus* control; #, $p < 0.05$ *versus* Cer 6:0).

cells to CS concomitant with treatment with ceramide synthesis inhibitors. The choice of ceramide species was based on solubility (species containing shorter length fatty acid chains being more soluble) and relevance (species containing longer length fatty-acid chains being more abundant in mammalian cells). For most treatments we utilized C6:0 ceramide. To ensure that this is a physiologically relevant ceramide, ceramide species were measured in the human acellular BAL that contained a vast range of ceramide species, including the short chain ceramide C6:0 (Cer C6:0) (Fig. 1*A*). Treatment of primary human AM collected via BAL from healthy volunteers with Cer C6:0 prior to co-culture with target apoptotic (UV-irradiated) Jurkat cells significantly inhibited human AM efferocytosis, measured by counting engulfed PI-labeled apoptotic cells on coded slides (Fig. 1*B*). Similarly, primary rat AM obtained via BAL from adult rats were pretreated with Cer C6:0 in dose-dependent and kinetic experiments (1, 5, and 10 μM for 1, 2, 4, and 18 h) prior to co-culture with target apo-

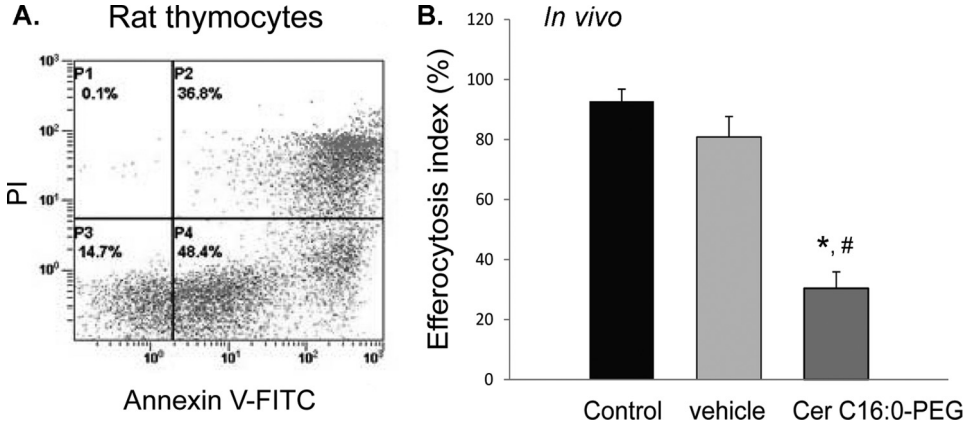

FIGURE 2. **Ceramide inhibits AM efferocytosis *in vivo*.** *A*, apoptosis of target thymocytes following *ex vivo* incubation (24 h), measured by flow cytometry following dual staining with PI and annexin V (representative flow panel; cells in the *right upper* and *right lower panels* are apoptotic). *B*, *in vivo* AM efferocytosis of intratracheally delivered PI-labeled apoptotic thymocytes (30 min), assessed by flow cytometry. AM were recovered by BAL from Sprague-Dawley rats treated intratracheally with either Cer 16:0 (PEG 2000-conjugated; 10 mg/kg; 24 h) or vehicle (PEG 2000); means ± S.E.; $n = 4$; *, $p < 0.05$ *versus* untreated; #, $p < 0.05$ *versus* vehicle).

ptotic Jurkat cells. Cer C6:0 inhibited AM efferocytosis in a dose- and time-dependent manner (Fig. 1, *C* and *D*) by up to 50% ($p < 0.005$; 10 μM) without inducing AM apoptosis (18) (data not shown). Based on these data, a concentration of 10 μM ceramide applied for 4 h prior to apoptotic target challenging was employed for subsequent experiments. Furthermore, to study the specificity of the effect of ceramides on AM efferocytosis, the cells were treated with DHC, the immediate precursor of ceramide in the *de novo* synthesis pathway. This sphingolipid is biologically distinct, despite close structural characteristics to ceramide. In fact, DHC may actually oppose some of the the effects of ceramide on mitochondrial membranes (38). Indeed, in contrast to ceramide, DHC 6:0 had no inhibitory effect on AM efferocytosis (Fig. 1*C*). Similar to short chain ceramide, the natural brain ceramide extract (a mixture of long and very long chain ceramides) inhibited apoptotic cell uptake by AM, compared with the vehicle control (Fig. 1*E*). Although we could not detect AM cell death following treatment with any ceramide species, to rule out a general nonspecific toxic effect on AM, we investigated whether the inhibitory effect of ceramide on AM efferocytosis was reversible upon removing ceramide from the media. Rat primary AM were treated for 4 h with ceramide and then allowed to recover overnight in regular growth medium prior to efferocytosis assays. Previously ceramide-treated AM completely recovered their engulfment capacity (Fig. 1*F*) to levels similar to those of untreated AM. This suggests that the effect of Cer C6:0 on apoptotic cell uptake is not permanent. To confirm that endogenously generated ceramide is as capable as exogenous ceramides to inhibit efferocytosis, AM were treated with active neutral sphingomyelinase (from Bacillus cereus), which generates ceramide from sphingomyelin. The endogenous ceramide production in response to SMase treatment (0.3 and 0.5 units/ml for 4 h) recapitulated the effects of exogenous ceramide treatment, significantly inhibiting rat AM efferocytosis by more than 85% ($p < 0.001$) (Fig. 1*G*). Most biological effects observed after the exogenous delivery of any ceramide species have been attributed to the generation of intracellular ceramides (39). We assessed, using specific inhibitors, the degree to which endogenous *versus* exogenous ceramides affected AM efferocytosis in response to short chain ceramide treatments (which could be mimicking increased pools of paracellular ceramide in pathological conditions, such as with CS). Both C6:0 and C8:0 ceramides required the activation of SPT in the *de novo* ceramide synthesis pathway to inhibit AM engulfment (Fig. 1*H* and data not shown, respectively), suggesting an early conversion of the exogenous ceramides to endogenous ceramides.

Ceramide Inhibits AM Efferocytosis in Vivo—In a model of *in vivo* AM efferocytosis, adult rats were treated intratracheally with target PI-labeled apoptotic thymocytes (Fig. 2*A*), followed 30 min later by investigation of apoptotic cell phagocytosis by resident AM collected by BAL. To investigate the effect of excessive ceramides on efferocytosis *in vivo*, lung ceramides were augmented by direct intratracheal application of the sphingolipid, as described previously in mice (17) using parameters (10 mg/kg) shown to cause lung parenchyma cell apoptosis and airspace enlargement (17, 34). To avoid potential toxicity of the usual ceramide vehicle (ethanol), we utilized a PEG-conjugated Cer C16:0, one of the most abundant ceramide species in the lung (as shown in Fig. 1*A*). Rats received Cer C16:0 or vehicle only (PEG 2000) followed 24 h later by intratracheal instillation of target PI-labeled apoptotic thymocytes. Compared with AM harvested from the BAL of untreated or vehicle-treated rats, resident AM from ceramide-treated animals demonstrated significantly decreased ability to engulf apoptotic thymocytes (Fig. 2*B*).

Ceramide Mediates the CS Effects on AM—CS is a potent inhibitor of AM efferocytosis (40). CS extract inhibited primary rat AM efferocytosis in a dose-dependent manner (Fig. 3*A*) as early as 1 h, but with a marked and significant effect after 4 h of treatment (Fig. 3*B*). This inhibitory effect persisted for up to 24 h after removal of cells from the CS-containing medium (Figs. 3*E* and 4*B*). Although CS exposure increases ceramides in the whole lung and in lung endothelial and epithelial cells in culture conditions (17), it remains unknown whether CS specifically up-regulates ceramides in AM. Primary rat AM were exposed to CS extract (1–10% v/v) fol-

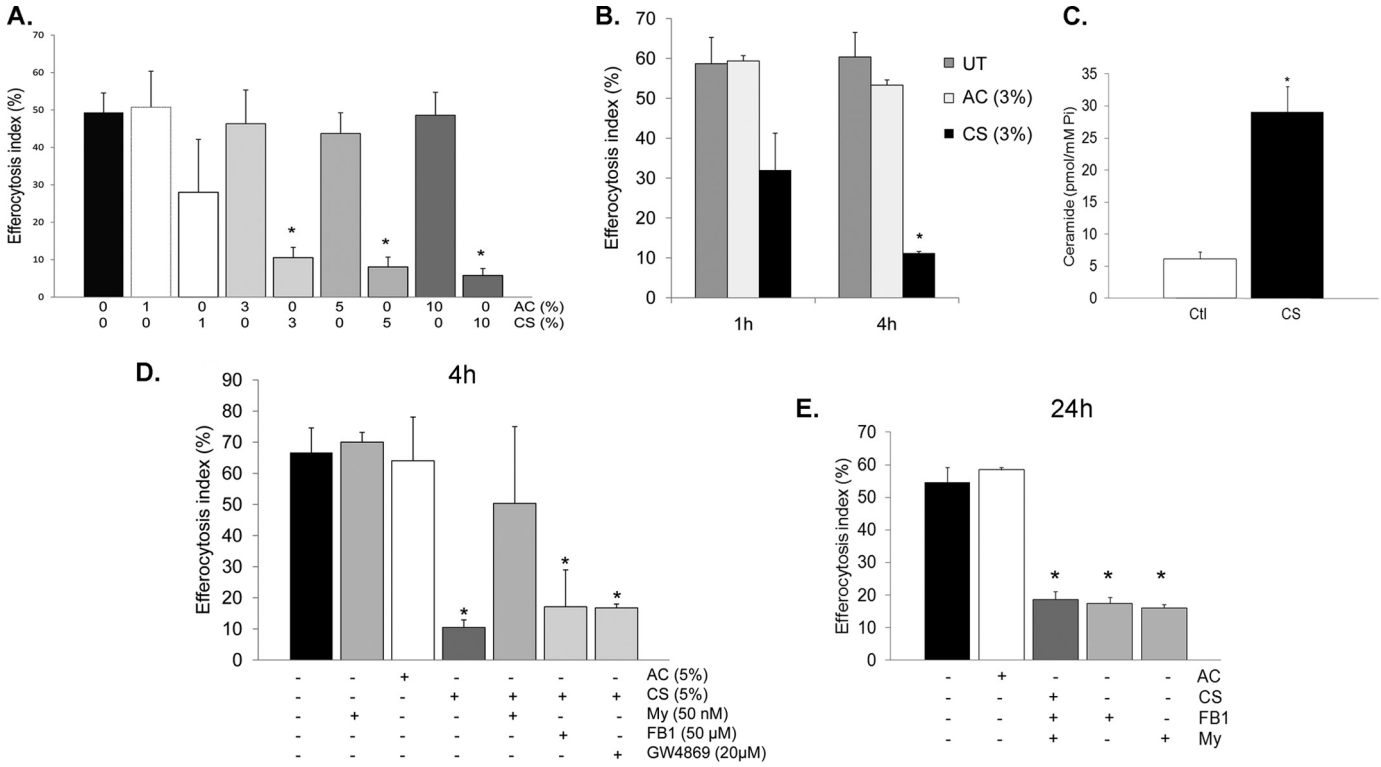

FIGURE 3. **CS inhibits AM efferocytosis in part by *de novo* ceramide synthesis via SPT.** *A*, effect of aqueous extract of ambient AC or CS (1, 3, 5, and 10% v:v; 4 h) on rat AM efferocytosis, measured by flow cytometry (means ± S.E.; $n = 10$; *, $p < 0.005$ *versus* control). *B*, time-dependent effects of CS (3% CS extract v:v) on rat AM efferocytosis, measured by flow cytometry; means ± S.E.; $n = 3$; *, $p < 0.05$ *versus* untreated control (*UT*). *C*, total ceramides 24 h after removal of rat AM from treatment with CS (3%; 4 h), measured by tandem mass spectrometry, followed by normalization by intracellular inorganic phosphorus content; means ± S.E.; $n = 4$; *, $p < 0.01$ *versus* control. *D* and *E*, rat AM efferocytosis of PI-labeled apoptotic Jurkat cells following CS exposure (3–5%; 4 h) and specific ceramide synthesis inhibitors myriocin (*My*; 50 nM; 2 h), fumonisin (*FB1*; 5 μM; 2 h), or GW4869 (20 μM; 30 min). Engulfment was assessed after 4 h of CS exposure (*D*) or 24 h after removal of AM from the CS treatment (*E*) and quantified by flow cytometry (means ± S.E.; $n = 3$; *, $p < 0.05$ *versus* AC).

lowed by lipid extraction and ceramide quantification via tandem mass spectrometry. There was an almost 2-fold increase in endogenous ceramides upon 4 h of CS exposure (acute response) ($n = 3$; $p = 0.03$), along with an increase in the production of DHC species (data not shown). Interestingly, the increase in ceramides continued even 24 h after removal of AM from the CS-containing medium, reaching a 5-fold increase (chronic response) (Fig. 3*C*). To investigate whether ceramide synthesis was necessary for the effect of CS on AM efferocytosis, AM were treated with specific ceramide synthesis inhibitors prior to CS extract exposure, followed by functional assessment of efferocytosis. Treatment with the *de novo* SPT inhibitor (myriocin; 50 nM; 2 h), but not with inhibitors of acid SMase (imipramine; 50 μM; 1 h) or neutral SMase (GW4869; 20 μM; 30 min) had a protective effect on AM, opposing the acute effects of CS on efferocytosis (Fig. 3*D*), but was ineffective on the more chronic effects of CS (Fig. 3*E*). Interestingly, fumonisin B1 (FB1; 50 μM; 2 h), which inhibits ceramide synthases in both the *de novo* pathway and the recycling pathway, did not mimic the effects of myriocin (Fig. 3*D*), suggesting that accumulation of sphingosine in response to FB1 may counteract its beneficial effects on inhibiting *de novo* ceramide synthesis (schematic in supplemental Fig. S1) in response to CS.

CS Impairs AM Efferocytosis through Sphingosine Accumulation—Ceramide deacylation via ceramidase generates sphingosine, which is a substrate for sphingosine kinases 1 and 2 to form sphingosine-1-phosphate (S1P) (schematic in supplemental Fig. S1). The role of sphingosine in phagocytosis is not known, but S1P has been reportedly involved in mycobacteria phagocytosis and is released upon engulfment of apoptotic cells (41, 42). We next investigated the role of ceramidase-mediated hydrolysis of ceramide to sphingosine in AM efferocytosis. Treatment of rat AM with the ceramidase inhibitor MAPP (1 μM; 2 h) followed by exposure to CS (3%; 4 h), although not affecting efferocytosis at 4 h, caused a marked protective effect against CS on AM efferocytosis at 24 h (Fig. 4, *A* and *B*). In addition, treatment with sphingosine (4 h) had a dose-dependent inhibitory effect on AM apoptotic clearance (Fig. 4*C*), whereas similar concentrations of S1P (4 h) had negligible effects on rat AM efferocytosis (Fig. 4*C*, *inset*, and data not shown). Treatment with the ceramide synthases inhibitor FB1 failed to rescue sphingosine-induced inhibition (Fig. 4*D*), whereas the ceramidase inhibitor MAPP rescued ceramide-induced blockage of efferocytosis (Fig. 4*E*), indicating that the effects of sphingosine were not due to generation of ceramide by ceramide synthase and that sphingosine is the principal mediator of the effect of ceramide on apoptotic cell engulfment. Together, these data suggest that CS inhibits apoptotic clearance in AM through ceramide deacylation to form sphingosine. We next investigated which of the two ceramidases, acid or neutral, mediates this inhibitory effect. Knockdown of acid ceramidase (ASAH1) via transient transfection of primary

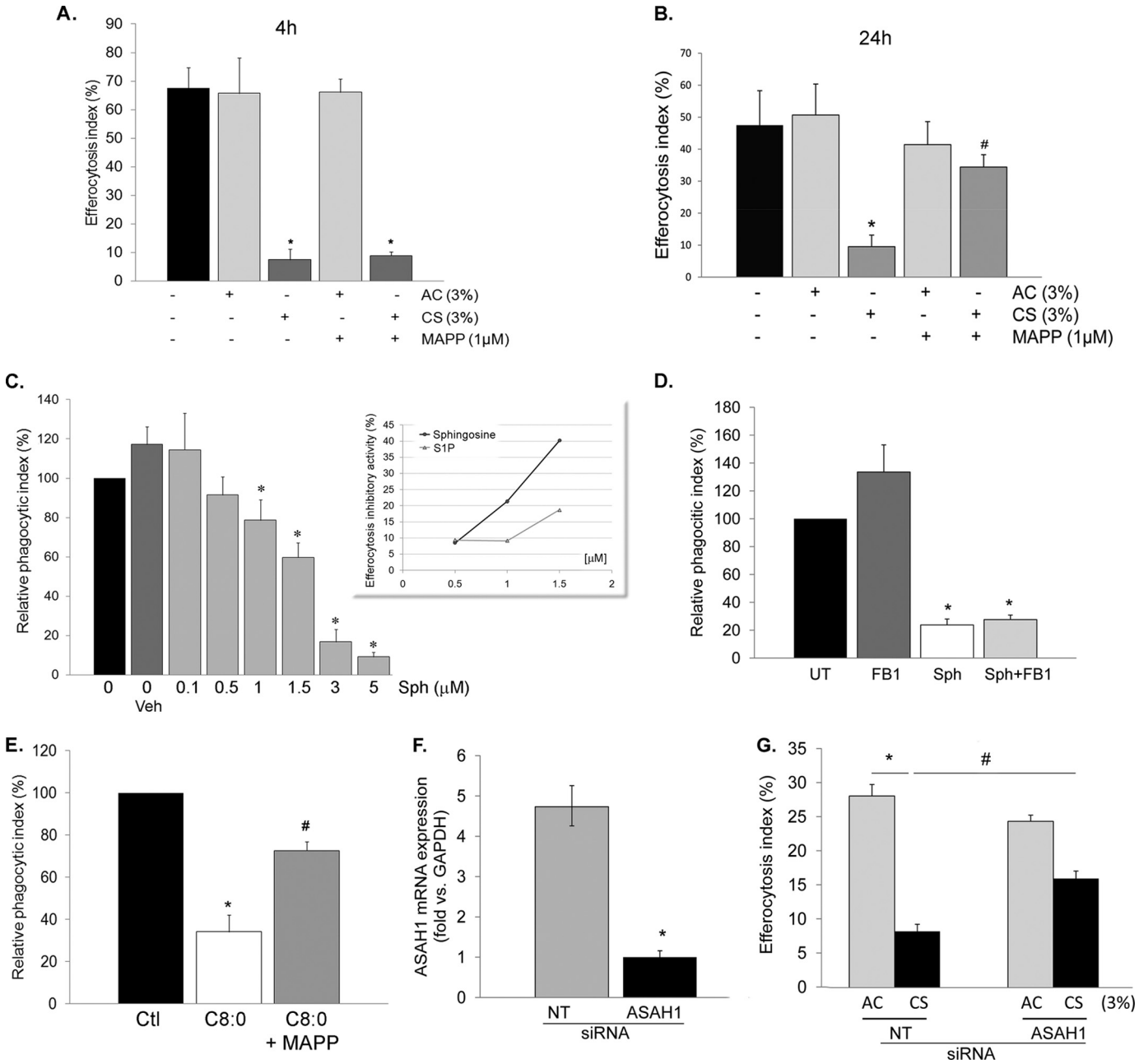

FIGURE 4. **CS inhibition of AM efferocytosis is sphingosine-dependent.** *A* and *B*, rat AM efferocytosis following inhibition of sphingosine synthesis with the ceramidase inhibitor (MAPP; 1 μM, 2 h) and exposure to CS (3%; 4 h) assessed immediately (*A*) or 24 h following removal of AM from the CS treatment (*B*) (means ± S.E.; *, $p < 0.05$ *versus* untreated control cells; #, $p < 0.05$ *versus* CS; $n = 4$). *C*, rat AM efferocytosis after treatment with sphingosine (*Sph*) at the indicated concentrations (4 h) or methanol vehicle (*Veh*; 0.7%; 4 h; means ± S.E.; $n = 3$; *, $p < 0.001$ *versus* untreated). *Inset*, inhibitory effect on efferocytosis (%) of sphingosine and S1P treatment at the indicated concentrations (4 h) on AM efferocytosis. *D*, rat AM efferocytosis following treatment (4 h) with ceramide synthase inhibitor fumonisin B1 (FB1; 5 μM; 2 h), sphingosine (3 μM), or sphingosine (3 μM) in the presence of FB1 (means ± S.E.; $n = 3$; *, $p < 0.05$ *versus* untreated (*UT*) control). *E*, AM efferocytosis after treatment with ceramide C8:0 (10 μM, 4 h) and the ceramidase inhibitor MAPP (1 μM, 2 h; mean ± S.E.; *, $p < 0.05$ *versus* untreated control; #, $p < 0.05$ *versus* C8:0; $n = 3$). *F*, acid ceramidase (ASAH1) mRNA expression (relative to GAPDH) measured in primary rat AM by real time PCR after 72 h of transient transfection with siRNA targeting ASAH1 (1 μM) or with nontarget siRNA (*NT*) (means ± S.D.; *, $p < 0.005$ *versus* NT siRNA; $n = 2$). *G*, rat AM efferocytosis following inhibition of sphingosine synthesis with acid ceramidase siRNA (1 μM, 72 h) and exposure to CS (3%; 4 h) or AC, assessed 24 h after removal of AM from the CS treatment (means ± S.E.; *, $p < 0.05$ *versus* control; #, $p < 0.05$ *versus* CS/NT; $n = 2$).

rat AM with specific siRNA (Fig. 4*F*) significantly rescued efferocytosis from CS inhibition (Fig. 4*G*), pointing out the role of this enzyme in sphingosine generation upon CS exposure. In contrast, neutral ceramidase gene knockdown by specific siRNA had no effect on the efferocytosis inhibition induced by CS (data not shown).

Rac1 Involvement in the CS and Effects of Ceramides on AM Efferocytosis—Treatment of AM with CS extract caused changes in the actin cytoskeleton, in particular a decrease in membrane ruffle formation, as visualized by fluorescence microscopy of Texas Red phalloidin staining (Fig. 5*A*). Given the central role of Rho GTPases in the unique regulation of effe-

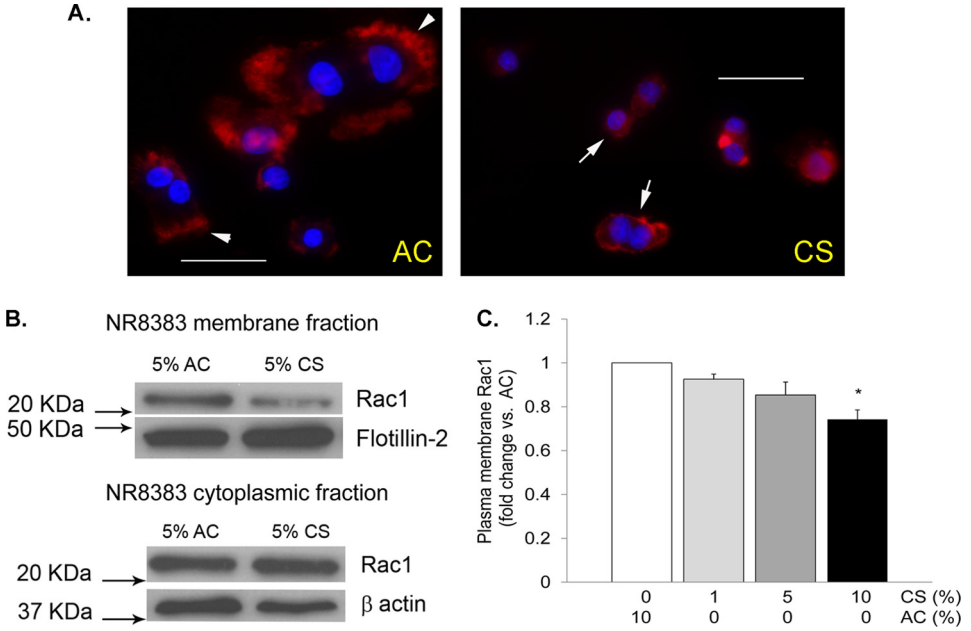

FIGURE 5. **CS decreases Rac1 membrane abundance.** *A*, representative fluorescence micrographs of AM (NR8383 cells) stained for actin (with Texas Red phalloidin; *red*) and nuclei (DAPI; *blue*) following treatment with AC or CS extract (5%; 4 h). Note that control cells (*left panel*) exhibit pronounced ruffling of the plasma membrane (*arrows*), whereas CS-treated cells (*right panel*) have markedly reduced membrane ruffle formation. *Scale bar*, 50 μm. *B*, Rac1 membrane abundance detected in protein lysates from total membrane and cytoplasmic fractions obtained from NR8383 cells treated with CS extract (5%; 4 h) or AC. The proteins were detected by Western blotting using a specific Rac1 antibody; flotillin-2 and β-actin were used as loading controls. *C*, densitometry of Rac1 expression detected by Western blotting normalized by loading control, expressed as fold change *versus* AC control (means ± S.E.; $n = 3$; *, $p <$ 0.05 *versus* AC).

rocytosis as compared with other types of phagocytosis and the role of Rac1 in membrane ruffling, we studied the effect of CS on the intracellular distribution of Rac1. AM were treated with CS extract (5%; 4 h) or control air extract, followed by cell fractionation and Rac1 immunoblotting of the cytoplasmic and the membrane fractions. CS markedly decreased the abundance of Rac1 in the plasma membrane fraction, as detected by immunoblotting with a Rac1-specific antibody (Fig. 5, *B* and *C*).

To determine whether treatment with ceramide recapitulates the effects of CS on the cytoskeleton and Rac1, AM were treated with ceramide (Cer C6:0; 10 μM; 4 h) and stained for actin and Rac1. AM treated with ceramide but not with vehicle exhibited marked changes in the actin cytoskeleton, notably a decrease in membrane ruffle formation (Fig. 6*A*), and a decrease in Rac1 at the plasma membrane, noted by immunocytochemistry using Rac1-specific antibody (Fig. 6*A*). Although a decrease in Rac1 is known to inhibit macrophage efferocytosis (43, 44), a similar effect could be achieved by an increase in RhoA, another Rho GTPase. Because ceramide treatment (Cer C6:0; 10 μM; 1 min, 3 min, 6 min, 12 min, 30 min, and 4 h) did not activate RhoA and treatment with a specific Rho kinase inhibitor (Y27632; 10 μM; 1 h) had no protective effect against ceramide-inhibited efferocytosis (data not shown), we next investigated whether Rac1 was mechanistically involved in the effect of ceramide on efferocytosis. AM were transfected with a constitutively active GFP-expressing Rac1 construct or with a control GFP-expressing plasmid prior to efferocytosis assays (Fig. 6*B*). In contrast to their effect on wild type AM (Figs. 1 and 2), ceramide treatment did not inhibit efferocytosis in AM expressing a constitutively active Rac1 (Fig. 6*C*). To link the ceramide pathway to the effect of CS on Rac1, sphingosine production was inhibited with the ceramidase inhibitor MAPP, which significantly restored the Rac1 abundance in the plasma membrane fraction of AM treated with CS (Fig. 6*D*).

DISCUSSION

Our results demonstrate a previously unappreciated function of ceramides in the inhibition of apoptotic cell clearance by human and rat alveolar macrophages *in vitro* and *in vivo*. This effect may have clinical relevance to the pathogenesis of emphysema. The efferocytosis responses of rat primary AM exposed *ex vivo* to CS extract are of similar magnitude and kinetics as those from AM isolated after *in vivo* exposure of C67/B6 mice to CS (40), suggesting that our model is consistent with *in vivo* events during CS-induced emphysema. The net loss of parenchymal cells via apoptosis is now recognized as a major component of emphysema pathogenesis, along with an inflammatory response causing protease/anti-protease imbalance with ensuing matrix proteolysis (45) and oxidative stress (46). The processes that explain the coexistence of excessive apoptosis with inflammation in the lung are not fully explained, because normally, apoptotic cells are rapidly cleared by specialized cells. Their persistence could lead to secondary necrosis and engagement of inflammatory responses. Chronic obstructive pulmonary disease patients display increased numbers of apoptotic cells in the lungs, which can be a consequence of both increased cell death (2, 4) and decreased apoptotic cell clearance (11, 47, 48). Previous investigations of the molecular mechanisms of excessive lung cell apoptosis led us to identify increases in ceramide species in

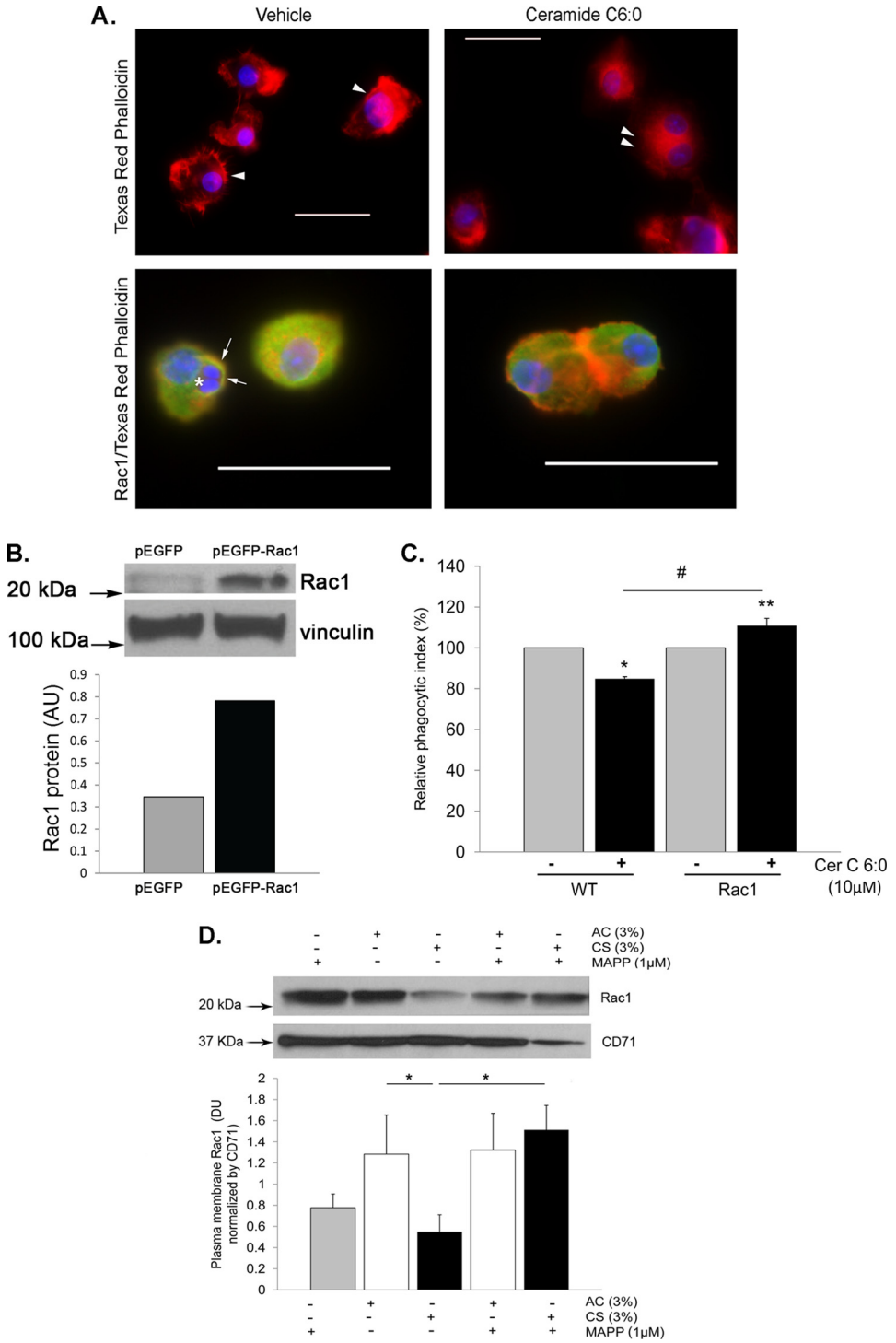

FIGURE 6. **Ceramide inhibits AM efferocytosis through Rac1 down-regulation.** *A*, representative fluorescence micrographs of AM (either alone in the *upper panels* or co-incubated with apoptotic Jurkat cells in the *lower panels*) stained for actin (with Texas Red phalloidin; *red*), nuclear marker (DAPI; *blue*), and Rac1 (with Rac1 antibody conjugated to Alexa fluor 488; *green*; *lower panels* only) following treatment with Cer C6:0 (10 μM; 4 h) or control vehicle (0.1% ethanol). Note that control cells exhibit ruffles of the plasma membrane (*arrows*), whereas ceramide-treated cells have a near loss of membrane ruffle formation (*double arrowhead*) and decreased Rac1 staining. The engulfed Jurkat apoptotic cells are seen in control cells (*asterisk*), surrounded by a Rac1-rich phagosome membrane (*arrow*). *Scale bar*, 50 μm. The values are representative of $n = 2$ experiments. *B*, Rac1 protein level in NR8383 cells transfected with constitutive active Rac1 or control plasmid. Vinculin immunoblot was used as loading control. *C*, phagocytic index of wild type NR8383 macrophages and those overexpressing Rac1 treated with ceramide (Cer C6:0; 10 μM; 4 h); note the lack of inhibitory effect of ceramide on efferocytosis in cells expressing a constitutively active Rac1 (means ± S.E.; $n = 3$). *D*, Rac1 plasma membrane abundance detected in protein lysates from total membrane fractions obtained from NR8383 cells treated with CS extract (3%; 4 h) or AC with or without a ceramidase inhibitor pretreatment (MAPP; 1 μM, 2 h). The proteins were detected by Western blotting using a specific Rac1 antibody, CD71 was used as loading control; densitometry of Rac1 expression was normalized by loading control (means ± S.E.; $n = 3$; *, $p < 0.05$).

the lungs of patients with emphysema (17). Endogenous ceramide synthesis can be stimulated by a variety of factors, including directly by CS (17, 34, 49). In addition, synthesis of ceramide species at the plasma membrane may lead to their release in the paracellular milieu where they can affect surrounding cells in a paracrine and/or autocrine manner. Our data suggest that multiple species of ceramides present in the lung exhibit similar effects on efferocytosis. Together with our previous reports of ceramide-mediated alveolar epithelial and endothelial cell apoptosis (17), our current data support the notion that ceramides may be molecular mediators of both structural cell apoptosis and alveolar macrophage efferocytosis impairment in the emphysematous lung. The effect of ceramide on AM efferocytosis was reversible upon cell removal from ceramide treatment. This result suggested that ceramides have a specific effect on efferocytosis function rather than a toxic effect on the macrophages. In fact, AM were found to be particularly resistant to the pro-apoptotic effects of ceramides (50), in contrast to lung structural cells (39). As expected, the exogenously added ceramides generated both endogenous *de novo* ceramides, which inhibited efferocytosis early in the time course, and sphingosine, which was responsible for late inhibitory effects on apoptotic cell engulfment. The involvement of ceramide up-regulation in CS-induced AM efferocytosis impairment adds an important piece to the puzzle of the molecular mediators and mechanisms by which CS exerts its action. Our results showed that SPT-mediated *de novo* ceramide synthesis followed by deacylation via acid ceramidase are important steps in the CS-mediated effect on AM efferocytosis, implicating for the first time the ceramide metabolite sphingosine as a key mediator of this biological process. These results emphasize the complexity of sphingolipid involvement in the regulation of various types of phagocytosis. For example, ceramide metabolites such as galactocerebroside, but not glucocerebroside, enhanced phagocytosis by neutrophils (51), and ceramide 1-phosphate was involved in phagosome formation (52), whereas S1P is involved in mycobacteria phagocytosis and may contribute to macrophage responses that follow the engulfment of apoptotic cells (41, 42).

The efferocytosis mechanism requires recognition of targets by the phagocyte followed by cytoskeletal reorganization and internalization of the target. The best studied "eat me" recognition signal is the exposure of phosphatidylserine (normally found on the inner leaflet of the plasma membrane) on the outer leaflet of the plasma membrane (53). We could not detect any effect of ceramide on the target recognition, as evaluated by the attachment index, or on the expression of the phosphatidylserine receptor in AM (data not shown). In turn, the Rac1 GTPase family protein was a major target of AM efferocytosis impairment by ceramides. The Rho family GTPases are known to regulate multiple signaling pathways that play a key role in the cytoskeleton organization (54). Rac1 promotes membrane ruffling and phagosome closure (55), and mutations of ced-10/Rac1 cause failure of phagocytosis of cell corpses after programmed cell death (43, 44), with Rac1-null macrophages exhibiting defective lamellipodium extension (56). In contrast, increased Rac1 activation promotes membrane ruffling that is necessary to facilitate uptake at the phagocytic cup and that decreases stress fiber formation, thus allowing for cell shape changes during engulfment. Although ceramide treatment did not stimulate RhoA activity, it had a marked effect on Rac1, like CS, by decreasing its abundance at the plasma membrane. These findings are consistent with previous studies of Rho family GTPase involvement in the CS effects on AM efferocytosis (40), where CS had no effect on RhoA activation immediately after exposure, activating it only at 24 h. These data, along with the observation of persistent inhibitory effects of CS on efferocytosis, suggest that CS may act on the interchange activation of Rac1 and RhoA proteins, early on by inhibiting ruffles formation via ceramide- and sphingosine-mediated Rac1 redistribution and at later time points by enabling stress fiber formation. Our work does not exclude additional targets of ceramide-induced effects on efferocytosis, including redox changes from reactive oxygen species production and modulation of other cytoskeletal events. Future studies will also have to address the molecular mechanism by which sphingosine impacts Rac1 plasma membrane interactions and the effect of ceramides on Fcγ-mediated AM phagocytosis. In conclusion, ceramides, which are found to be up-regulated in response to CS, and their deacylation product sphingosine dose-dependently impair AM efferocytosis, both directly in a paracellular context and as second messengers of CS exposure.

Acknowledgments—We acknowledge Amanda Fisher, Marjorie Albrecht, and Ioan S. Chesches for expert technical assistance, and we thank Peter Henson for advice and support.

REFERENCES

1. Yoshida, T., and Tuder, R. M. (2007) *Physiol. Rev.* **87,** 1047–1082
2. Kasahara, Y., Tuder, R. M., Taraseviciene-Stewart, L., Le Cras, T. D., Abman, S., Hirth, P. K., Waltenberger, J., and Voelkel, N. F. (2000) *J. Clin. Invest.* **106,** 1311–1319
3. Tuder, R. M., Petrache, I., Elias, J. A., Voelkel, N. F., and Henson, P. M. (2003) *Am. J. Respir. Cell Mol. Biol.* **28,** 551–554
4. Tuder, R. M., Zhen, L., Cho, C. Y., Taraseviciene-Stewart, L., Kasahara, Y., Salvemini, D., Voelkel, N. F., and Flores, S. C. (2003) *Am. J. Respir. Cell Mol. Biol.* **29,** 88–97
5. Rangasamy, T., Cho, C. Y., Thimmulappa, R. K., Zhen, L., Srisuma, S. S., Kensler, T. W., Yamamoto, M., Petrache, I., Tuder, R. M., and Biswal, S. (2004) *J. Clin. Invest.* **114,** 1248–1259
6. Henson, P. M., Bratton, D. L., and Fadok, V. A. (2001) *Nat. Rev. Mol. Cell Biol.* **2,** 627–633
7. Vandivier, R. W., Henson, P. M., and Douglas, I. S. (2006) *Chest* **129,** 1673–1682
8. Henson, P. M., and Tuder, R. M. (2008) *Am. J. Physiol. Lung Cell Mol. Physiol.* 4.L601–611
9. Kasahara, Y., Tuder, R. M., Cool, C. D., Lynch, D. A., Flores, S. C., and Voelkel, N. F. (2001) *Am. J. Respir. Crit. Care Med.* **163,** 737–744
10. Golpon, H. A., Fadok, V. A., Taraseviciene-Stewart, L., Scerbavicius, R., Sauer, C., Welte, T., Henson, P. M., and Voelkel, N. F. (2004) *FASEB J.* **18,** 1716–1718
11. Uller, L., Persson, C. G., and Erjefält, J. S. (2006) *Trends Pharmacol. Sci.* **27,** 461–466
12. Hodge, S., Hodge, G., Ahern, J., Jersmann, H., Holmes, M., and Reynolds, P. N. (2007) *Am. J. Respir. Cell Mol. Biol.* **37,** 748–755
13. Mathias, S., Peña, L. A., and Kolesnick, R. N. (1998) *Biochem. J.* **335,** 465–480
14. Spiegel, S., Foster, D., and Kolesnick, R. (1996) *Curr. Opin. Cell Biol.* **8,**

159–167
15. Merrill, A. H., Jr., Schmelz, E. M., Dillehay, D. L., Spiegel, S., Shayman, J. A., Schroeder, J. J., Riley, R. T., Voss, K. A., and Wang, E. (1997) *Toxicol. Appl. Pharmacol.* **142,** 208–225
16. Rosen, H., and Liao, J. (2003) *Curr. Opin. Chem. Biol.* **7,** 461–468
17. Petrache, I., Natarajan, V., Zhen, L., Medler, T. R., Richter, A. T., Cho, C., Hubbard, W. C., Berdyshev, E. V., and Tuder, R. M. (2005) *Nat. Med.* **11,** 491–498
18. Monick, M. M., Mallampalli, R. K., Carter, A. B., Flaherty, D. M., McCoy, D., Robeff, P. K., Peterson, M. W., and Hunninghake, G. W. (2001) *J. Immunol.* **167,** 5977–5985
19. Schramm, M., Herz, J., Haas, A., Krönke, M., and Utermöhlen, O. (2008) *Cell Microbiol.* **10,** 1839–1853
20. Utermöhlen, O., Karow, U., Löhler, J., and Krönke, M. (2003) *J. Immunol.* **170,** 2621–2628
21. Gómez-Muñoz, A. (2004) *FEBS Lett.* **562,** 5–10
22. Ridley, A. J. (2001) *Trends Cell Biol.* **11,** 471–477
23. Nakaya, M., Tanaka, M., Okabe, Y., Hanayama, R., and Nagata, S. (2006) *J. Biol. Chem.* **281,** 8836–8842
24. Hanna, A. N., Berthiaume, L. G., Kikuchi, Y., Begg, D., Bourgoin, S., and Brindley, D. N. (2001) *Mol. Biol. Cell* **12,** 3618–3630
25. Twigg, H. L., Soliman, D. M., Day, R. B., Knox, K. S., Anderson, R. J., Wilkes, D. S., and Schnizlein-Bick, C. T. (1999) *Am. J. Respir. Crit. Care Med.* **159,** 1439–1444
26. Lee, C. K., Park, H. J., So, H. H., Kim, H. J., Lee, K. S., Choi, W. S., Lee, H. M., Won, K. J., Yoon, T. J., Park, T. K., and Kim, B. (2006) *Proteomics* **6,** 6455–6475
27. Hed, J., Hallden, G., Johansson, S. G., and Larsson, P. (1987) *J. Immunol. Methods* **101,** 119–125
28. Pérez, R., Balboa, M. A., and Balsinde, J. (2006) *J. Immunol.* **176,** 2555–2561
29. Carp, H., and Janoff, A. (1980) *Exp. Lung Res.* **1,** 225–237
30. Bligh, E. G., and Dyer, W. J. (1959) *Can. J. Biochem. Physiol.* **37,** 911–917
31. Dobrowsky, R. T., and Kolesnick, R. N. (2001) *Methods Cell Biol.* **66,** 135–165
32. Petrache, I., Birukov, K., Zaiman, A. L., Crow, M. T., Deng, H., Wadgaonkar, R., Romer, L. H., and Garcia, J. G. (2003) *FASEB J.* **17,** 407–416
33. Bartke, N., and Hannun, Y. A. (2009) *J. Lipid Res.* **50,** (suppl.) S91–S96
34. Petrache, I., Medler, T. R., Richter, A. T., Kamocki, K., Chukwueke, U., Zhen, L., Gu, Y., Adamowicz, J., Schweitzer, K. S., Hubbard, W. C., Berdyshev, E. V., Lungarella, G., and Tuder, R. M. (2008) *Am. J. Physiol. Lung Cell Mol. Physiol.* **295,** L44–L53
35. Olivera, A., Buckley, N. E., and Spiegel, S. (1992) *J. Biol. Chem.* **267,** 26121–26127
36. Deigner, H. P., Claus, R., Bonaterra, G. A., Gehrke, C., Bibak, N., Blaess, M., Cantz, M., Metz, J., and Kinscherf, R. (2001) *FASEB J.* **15,** 807–814
37. Finnegan, C. M., Rawat, S. S., Puri, A., Wang, J. M., Ruscetti, F. W., and Blumenthal, R. (2004) *Proc. Natl. Acad. Sci. U.S.A.* **101,** 15452–15457
38. Szulc, Z. M., Bielawski, J., Gracz, H., Gustilo, M., Mayroo, N., Hannun, Y. A., Obeid, L. M., and Bielawska, A. (2006) *Bioorg. Med. Chem.* **14,** 7083–7104
39. Medler, T. R., Petrusca, D. N., Lee, P. J., Hubbard, W. C., Berdyshev, E. V., Skirball, J., Kamocki, K., Schuchman, E., Tuder, R. M., and Petrache, I. (2008) *Am. J. Respir. Cell Mol. Biol.* **38,** 639–646
40. Richens, T. R., Linderman, D. J., Horstmann, S. A., Lambert, C., Xiao, Y. Q., Keith, R. L., Boé, D. M., Morimoto, K., Bowler, R. P., Day, B. J., Janssen, W. J., Henson, P. M., and Vandivier, R. W. (2009) *Am. J. Respir. Crit. Care Med.* **179,** 1011–1021
41. Thompson, C. R., Iyer, S. S., Melrose, N., VanOosten, R., Johnson, K., Pitson, S. M., Obeid, L. M., and Kusner, D. J. (2005) *J. Immunol.* **174,** 3551–3561
42. Weigert, A., Johann, A. M., von Knethen, A., Schmidt, H., Geisslinger, G., and Brüne, B. (2006) *Blood* **108,** 1635–1642
43. Ellis, R. E., Jacobson, D. M., and Horvitz, H. R. (1991) *Genetics* **129,** 79–94
44. Reddien, P. W., and Horvitz, H. R. (2000) *Nat. Cell Biol.* **2,** 131–136
45. Demedts, I. K., Brusselle, G. G., Bracke, K. R., Vermaelen, K. Y., and Pauwels, R. A. (2005) *Curr. Opin. Pharmacol.* **5,** 257–263
46. Barnes, P. J., Shapiro, S. D., and Pauwels, R. A. (2003) *Eur. Respir. J.* **22,** 672–688
47. Hodge, S., Hodge, G., Scicchitano, R., Reynolds, P. N., and Holmes, M. (2003) *Immunol. Cell Biol.* **81,** 289–296
48. Vandivier, R. W., Fadok, V. A., Hoffmann, P. R., Bratton, D. L., Penvari, C., Brown, K. K., Brain, J. D., Accurso, F. J., and Henson, P. M. (2002) *J. Clin. Invest.* **109,** 661–670
49. Levy, M., Khan, E., Careaga, M., and Goldkorn, T. (2009) *Am. J. Physiol. Lung Cell Mol. Physiol.* **297,** L125–L133
50. Monick, M. M., Carter, A. B., Gudmundsson, G., Geist, L. J., and Hunninghake, G. W. (1998) *Am. J. Physiol.* **275,** L389–L397
51. Sakai, M., Nagasawa, S., and Takahashi, K. (2000) *Biochem. Biophys. Res. Commun.* **278,** 79–83
52. Hinkovska-Galcheva, V., Boxer, L. A., Kindzelskii, A., Hiraoka, M., Abe, A., Goparju, S., Spiegel, S., Petty, H. R., and Shayman, J. A. (2005) *J. Biol. Chem.* **280,** 26612–26621
53. Fadok, V. A., Bratton, D. L., Frasch, S. C., Warner, M. L., and Henson, P. M. (1998) *Cell Death Differ* **5,** 551–562
54. Bosco, E. E., Mulloy, J. C., and Zheng, Y. (2009) *Cell Mol. Life Sci.* **66,** 370–374
55. Chimini, G., and Chavrier, P. (2000) *Nat. Cell Biol.* **2,** E191–E196
56. Heasman, S. J., and Ridley, A. J. (2008) *Nat. Rev. Mol. Cell Biol.* **9,** 690–701